Determination of the overall heat transmission coefficient (u-value) of vacuum glazing

Simko, T. M.; Elmahdy, A. H.; Collins, R. E.

Publisher's version / Version de l'éditeur:

ASHRAE Transactions, 105, pt. 2, pp. 1-9, 1999

Determination of the overall heat transmission coefficient (U-Value) of vacuum glazing

Simko, T.M.; Elmahdy, A.H.; Collins, R.E.

NRCC-41907

A version of this document is published in / Une version de ce document se trouve dans :
ASHRAE Transactions, v. 105, pt. 2, 1999, pp. 1-9

DETERMINATION OF THE OVERALL HEAT TRANSMISSION COEFFICIENT (U-VALUE) OF VACUUM GLAZING

T. M. Simko*, A.H. Elmahdy† and R. E. Collins*

*School of Physics, University of Sydney, NSW 2006, Australia

†Institute for Research in Construction, National Research Council of Canada, Ottawa, Canada

ABSTRACT

The heat flow through a 1 m × 1 m sample of vacuum glazing has been measured in two independent ways. One measurement method uses a guarded hot box to make a direct determination of overall heat transmission coefficient under standard test conditions. The other method uses a small area guarded hot plate (specially designed for this purpose) to measure the local radiative and (negligible) gas conductance between the glass sheets. This instrument is also used to validate calculations of the heat flow through the support pillars. The overall heat flow is then obtained by combining the contributions from these processes with those due to heat flow through the conducting edge seal. The results obtained with the two methods are in very good agreement for the same external conditions. These results provide the first independent validation of estimates of heat flow through vacuum glazing based on the five separate processes, which contribute to this heat transfer.

Key words: U-value, evacuated, glazing, heat transmission, testing, modelling.

INTRODUCTION

Vacuum glazing is a new form of transparent thermal insulator with the potential for application in windows. Collins and Simko (1998) recently reviewed this technology. Vacuum glazing consists of two plane sheets of glass, hermetically sealed together around the edges, and surrounding a narrow, highly evacuated space. The separation of the glass sheets under the influence of atmospheric pressure is maintained with an array of small, high strength support pillars. Radiative heat transfer between the internal surfaces of the glass sheets can be reduced to a low level by the incorporation of one, or two transparent low emissivity coating on these surfaces.

Vacuum glazing is not a new concept. Zoller (1924) first described it in a patent application filed in 1913, only 20 years after the invention of the Dewar flask. Despite many attempts, however, it is only in the last few years that there has been significant progress in developing this concept. The first samples of vacuum glazing with a thermally insulating internal vacuum were made at The University of Sydney, Australia (UNSA) less than a decade ago, as reported by Robinson and

Collins (1989). Since that time, over 700 samples of vacuum glazing have been made by this group, using a construction shown schematically in Figure 1. The UNSA design uses solder glass to make the hermetic edge seal between two sheets of three or 4 mm thick soda lime glass. During the process to make the edge seal, the entire structure is heated to temperatures around 450°C, at which the solder glass melts and fuses to the surfaces of the glass sheets. The only transparent low emittance coatings which have been found to survive the high temperature edge seal process are pyrolytically deposited (hard coat) doped tin oxide (Pilkington, 1989). The support pillars are usually made from metal, are typically 0.25 to 0.5 mm in diameter, and separated by 20 to 25 mm. Vacuum glazing has been made in the laboratory in sizes up to 1 m × 1 m with air-to-air, center of glazing U-values as low as 0.80 W/(m^2 K). A good understanding has been obtained of the physical mechanisms, which can lead to heat flow through the glazing, and of the ways in which mechanical stress can arise in these devices. Methods have been developed for designing vacuum glazing which quantify the tradeoffs between reducing heat flow through the glazing (which requires fewer and smaller pillars), and decreasing mechanical stresses in the glazing (which leads to the need for more and larger pillars).

This paper is concerned with heat transfer through vacuum glazing. Heat flow through this type of glazing is influenced by several different processes, including: heat transfer between the external glass surfaces and the environment; gaseous conduction and radiative heat transfer between the internal surfaces of the glass sheets; thermal conduction through the mechanical support pillars; and lateral heat flow along the glass sheets in the vicinity of the edge seal. Each of these processes is discussed, and techniques are described for determining their magnitudes and the influence of effects associated with their interaction.

Two methods are described for measuring the overall heat flow through vacuum glazing. In one method, measurements of *total* heat flow are made through a large area (1 m × 1 m) sample of vacuum glazing in an accurately characterized guarded hot box under well defined boundary conditions. In the other method, the *local* heat flow through the glazing due to radiation and residual gas conduction is measured in a small, pillar-free region with a specially designed guarded hot plate apparatus. The overall heat flow is estimated by combining this heat flow with experimentally validated modelling data for heat flow through the support pillars and in the vicinity of the relatively highly conducting edge seal, under the influence of similar boundary conditions. The results obtained with both methods are shown to be in excellent agreement.

2. HEAT TRANSFER PROCESSES IN VACUUM GLAZING

In this section, the different processes, which can cause heat to flow through vacuum glazing, are discussed. Where appropriate, comment is made on the way in which the heat flows due to these separate processes interact in order to determine the overall heat transfer through vacuum glazing.

2.1 EXTERNAL HEAT TRANSFER PROCESSES

Heat transfer to and from the external surfaces of the glazing involves a combination of forced and natural convection, and radiation. As in most treatments of such heat transfer process, the approach taken here is to characterize these external processes by a heat transfer coefficient h (W/(m^2 K)) for each side. The heat flow Q (W) through area A (m^2) for an air-to-glass temperature difference ΔT is thus written:

$$Q = hA\Delta T \tag{1}$$

The values of the external heat transfer coefficients, h, depend on the specific environmental conditions. The ASTM (1991) fenestration test standard gives values of 8.3 W/(m^2 K) and 30 W/(m^2 K) for the warm and cold sides of the glazing respectively for winter conditions. In this paper, we present data of heat flow through vacuum glazing for boundary heat transfer coefficients, which are quite close to these "standard" values.

2.2 GASEOUS CONDUCTION

Extensive studies have been undertaken which have shown that, for all well made samples of vacuum glazing, the gaseous conduction is negligible relative to the other heat flows mechanisms, and remains negligible after many years of storage at room, and somewhat elevated temperatures. Details of this work have been reported by Turner et al. (1994). Therefore, the contribution from gaseous conduction to the overall heat flow through the sample of vacuum glazing studied is ignored in the present study.

2.3 RADIATIVE HEAT FLOW

The net radiative heat flow between two plane parallel surfaces of area A (m^2) at temperatures T_1 (K) and T_2 (K) and having hemispherical emissivities e_1 and e_2 can be written as (assuming that the temperature drop across the glass sheets is negligible):

$$Q_{radiation} = e_{effective}\sigma A(T_1^4 - T_2^4) \tag{2}$$

where σ is the Stefan-Boltzmann constant (5.67×10^{-8} W/(m^2 K^4)). In Equation 2, the effective emittance, $e_{effective}$, is conventionally written as:

$$e_{effective} = \frac{1}{\frac{1}{e_1} + \frac{1}{e_2} - 1} \tag{3}$$

For temperatures that are not too different, radiative heat transfer coefficient, r (W/(m^2 K)), may be approximated by the following expression (using Taylor expansion):

$$r = 4e_{effective}\sigma\overline{T}^3 \tag{4}$$

where $\overline{T}$ is the average of the temperatures of the two surfaces.

Equation 3 is strictly speaking only valid for surfaces for which the reflectance is independent of wavelength and angle of incidence to the normal. No practical surface possesses such ideal properties. As noted by Zhang et al. (1997), an accurate calculation of radiative heat transfer between two surfaces therefore requires an integration over angle and wavelength of the black body spectra for the two surfaces, weighted by the effective angle and wavelength dependent emittance for these surfaces. As discussed below, such a procedure is essential in the calibration of the small area guarded hot plate apparatus. Zhang et al. (1997) have shown, however, that the simplistic Equation 2 provides an accurate representation of radiative heat transfer, including its temperature dependence, provided that the value of effective emittance is only slightly different from that obtained conventionally by combining the hemispherical emittances as in Equation 3. They further show that the effective emittance of clear, and doped tin oxide coated glass is essentially independent of temperature over the range -20°C to +20°C. In this work, the radiative heat transfer in the sample of vacuum glazing has been determined by direct experimental measurement for the surfaces at two specific temperatures. Equation 4 is then used to determine the radiative heat transfer coefficient at other temperatures, assuming an effective emittance, which is independent of temperature.

2.4 PILLAR CONDUCTION

As noted above, mechanical support pillars maintain the separation of the two glass sheets in vacuum glazing under the influence of the forces due to atmospheric pressure. These pillars also provide thermal bridging between the glass sheets, thus increasing the overall heat flow through the glazing. An estimate of the magnitude of the heat flow through an individual support pillar can be obtained from the classical expression for the thermal resistance associated with a small circular contact between two otherwise isolated semi-infinite slabs of material - in this case, the glass sheets. As shown by Holm (1979), the heat flow for this situation is:

$$Q_{one-pillar} = 2k_{glass}a(T_2 - T_1) \tag{5}$$

where k_{glass} is the thermal conductivity of the glass sheets (W/(m K)), a is the radius of the contact area (m), and T_1 and T_2 are the temperatures of the slabs at large distances from the contact.

Equation 5 assumes that all of the thermal resistance associated with the heat flow is in the glass sheets, and that the thermal resistance of the pillar itself is negligible. The metal pillars used in the sample of vacuum glazing have a thermal conductivity of about 45 W/(m K), which is much greater than that of glass (about 1.0 W/(m K)). This is, therefore, a very good approximation. Similarly, Equation 5 is based on the assumption that the glass sheets are infinite in extent. Using finite element methods, Simko (1996) has shown that, for pillars with diameters much less than the thickness of the glass sheets, Equation 5 does indeed provide an accurate estimate of the heat flow through a single pillar. This result has also been validated by experimental measurements on individual pillars using the small area guarded hot plate apparatus described below.

Simko (1996) has used finite element modelling methods to show that the heat flow through an individual pillar is essentially unaffected by the presence of all the other pillars in the array. The heat transfer coefficient due to conduction ($c_{pillar\text{-}array}$, W/(m^2 K)), of the whole pillar array can therefore be obtained by multiplying the conductance of each individual pillar $2k_{glass}a$, by the number of pillars per unit area $1/\lambda^2$, where λ (m) is the pillar separation:

$$c_{pillar-array} = 2k_{glass}a / \lambda^2 \tag{6}$$

Each highly conducting support pillar greatly alters the temperature of the inner surfaces of the glass sheets in its immediate vicinity. It might be thought that this would result in a significant reduction in the radiative heat transfer through the glazing. Simko (1996) has shown, however, that the effect of these temperature variations on the overall radiative heat transfer is virtually identical to that which would occur if the heat flow through the pillars were uniformly distributed over the internal surfaces of the glazing. To a very good approximation, therefore, heat flow due to the pillars and due to radiation can be combined additively.

The localization of the heat flow through each pillar results in small, but measurable temperature variations on the external surfaces of the glass sheets, for the usual boundary heat transfer coefficients. These variations are largest in the immediate vicinity of each pillar where the local heat flow density is about twice the average density for a typical value of pillar separation. In fact, over most of each unit cell of the pillar array, this heat flow per unit area at the external surface is reasonably uniform; a measurement of surface temperature at points remote from each pillar is therefore very close to that which would be obtained if the heat flow at the external surface were uniform. This point is important in the selection of the thermocouple positions used to determine the surface temperatures of the glass sheets in the guarded hot box measurements.

2.5 EDGE CONDUCTION

In vacuum glazing, as in all designs of insulating glass units, the heat flow per unit area near the edges of glass is larger than that remote from the edges. This occurs because heat flows laterally along the glass sheets and through the relatively highly conducting edge seal. A simple, one-dimensional analytic model has been developed by Simko et al. (1995) for estimating the magnitude of the heat flow through the edge seal of vacuum glazing units. In this model, temperature gradients *through* the thickness of the glass sheets are ignored. The heat flow is calculated for a pair of infinitesimal elements on opposite sides of the glazing due to three effects: heat transfer between the external environment and each element; heat transfer between the elements due to radiation and pillar conduction; and lateral heat flow along the glass sheets. In this calculation, the heat flows due to radiation and through the pillar array are simulated by incorporating in the model a uniform slab of material of appropriate thermal conductivity. External heat transfer is approximated by uniform heat transfer coefficients. The model leads to a pair of coupled, second order differential equations for the temperatures of the glass sheets on either side of the glazing. Continuity requires that these two temperatures, and their gradients, be equal at the edge of the glazing. The differential equations are solved easily using finite difference techniques.

In certain simple cases, an analytic expression can be obtained for the temperatures of the glass sheets and the heat flow through the edge seal. For example, for highly insulating glazing, it is found that the temperature on each side varies exponentially, approaching the center-of-glazing value with a characteristic distance of $(k_{glass}t/h)^{1/2}$, where k_{glass} is the thermal conductivity of glass, t is the thickness of either glass sheet, and h is the heat transfer coefficient at the external surface of the glass sheet [Simko, 1996]. This result can be used to show that the total heat flow per unit length of the edge seal from one side to the other is equal to that which would flow through a slab of glass of thickness t, and length equal to the sum of the characteristic distances on each side, for a temperature difference equal to that between the glass sheets remote from the edges. This analysis can be extended to a situation where thermal insulation extends over the glass sheets for some distance beyond the edge seal; in this case, the total insulated length is added to the sum of the characteristic distances to obtain the heat flow through the edge seal.

Because the highly conducting edge seal significantly reduces the temperature difference between the glass sheets in its vicinity, the heat flow between the glass sheets due to radiative and pillar conduction is also reduced in this region. An estimate of the magnitude of this effect can be obtained by considering the case of equal heat transfer coefficients on both sides. The reduction in this case is equal to the heat which would flow due to radiation and pillar conduction through a strip around the edges of the glazing, which is equal in width to one characteristic distance of the exponential temperature distribution.

Simko et al. (1995) have shown that temperatures obtained from the finite difference solution to the one-dimensional analytic model are in excellent agreement with results from a three-dimensional finite element model, and with independent infrared thermographic measurements on a sample of vacuum glazing.

2.6 TOTAL HEAT FLOW THROUGH VACUUM GLAZING

As noted above, the total heat transfer through the glazing can be calculated by solving the analytic model numerically using finite difference methods. This approach allows for slight departures from an exponential temperature dependence due to heat transfer within the glazing. It also automatically includes effects associated with reductions in radiation and pillar conduction due to the temperature gradients near the edge seal. In addition, and of particular relevance to this work, the finite difference method of solution permits inclusion of effects associated with additional heat flow through any uninsulated region of the solder glass edge seal.

It is also useful to obtain an approximate estimate of the total heat flow in terms of the separate processes, which contribute to this flow. In regions remote from the edge seal, the heat transfer coefficient due to radiation and pillar conduction simply add in parallel. The total heat flow in this region is then obtained from the series combination of thermal resistances associated with this heat flow, and with the external heat transfer processes. The heat flow along the glass sheets near the edges of the glazing can be estimated using the method described above, assuming that the glass temperature varies exponentially in this region. A correction can be included for the reduction in radiation and pillar conduction in the region of temperature non-uniformity near the edges.

3. MEASUREMENT METHODS

As noted above, two different experimental methods have been used in this work to measure the heat transfer through vacuum glazing. These methods have been described in detail elsewhere. In this section, a brief summary is presented of the important features of each method in the context of determining heat transfer through vacuum glazing.

3.1 SMALL AREA GUARDED HOT PLATE

The small area guarded hot plate was developed specifically to measure radiative heat transfer and gas conduction in vacuum glazing. This instrument, which operates on the same principle as a conventional guarded hot plate, is shown schematically in Figure 2. Heat flow from a small thermal conductor, referred to here as the metering piece, is determined by dissipating resistive power within it in order to bring its temperature into equality with a surrounding isothermal guard. A detailed description of this apparatus is given by Collins et al. (1993).

There are three key features of this instrument which warrant comment here. Firstly, the circular measurement area is quite small - only 13 mm in diameter. This is necessary because measurements of radiative and gaseous heat flow must be made in a pillar-free region of the sample, and there are fundamental stress-related limitations on the size of an unsupported area of 3 to 4 mm thick glass under the influence of forces due to atmospheric pressure. All experimental samples of vacuum glazing are made with a pillar-free region approximately 50 mm across. Modelling results from Collins et al. (1993) show that, for isothermal surfaces, the support pillars outside this region make a negligible contribution to the heat flow measured at the center of the region.

The second important design feature of the small area guarded hot plate relates to the nature of the sample to be measured. In vacuum glazing, the insulating region (the evacuated space) is located between two relatively highly conducting regions (the glass sheets). Great care is therefore necessary to eliminate parasitic heat flows due to lateral conduction along the glass sheets. Moreover, since the metering piece and the guarded region of the instrument are both in good thermal contact with one of the glass sheets of the glazing, they are also in good thermal contact with each other. In order to achieve adequate sensitivity in the identification of the null condition for the measurement of power, it is thus necessary to detect very small temperature differences between the metering piece and the guard. Small, high resistance thermistors are used in a bridge configuration in this instrument to detect temperature differences of 10^{-4} K. This corresponds to a power resolution of 10^{-5} W, or approximately 0.5% of the radiative heat transfer between two low emissivity (e = 0.2) surfaces for a temperature difference of 20°C.

Third, comment should be made on the calibration of this instrument. Due to its very small size, the area of the metering piece is not very precisely defined geometrically. It is therefore necessary to calibrate the effective area of the instrument by performing measurements on a sample for which the magnitude of the heat transfer is accurately known. The sample used for this purpose consists of two closely spaced, clear soda lime glass sheets, with a dynamically pumped internal volume. The pressure within the sample is below 10^{-2} Pa, so that gas conduction is negligible. The sheets are separated by support pillars that are sufficiently far removed from the measuring area that pillar conduction is essentially negligible. Heat transfer in this "standard sample" is therefore entirely by radiation between the two glass sheets. The radiative heat transfer coefficient is determined as discussed in Section 2.3 above, using the method described by Zhang et al. (1997). The validity of this calibration procedure has been demonstrated by comparison with measurements using a larger area (~50 mm diameter) guarded hot plate having an accurately known geometry. The accuracy of the small area guarded hot plate measurements of radiative and gas conductance on the test sample of vacuum glazing is estimated to be ±1%.

3.2 LARGE AREA CALIBRATED GUARDED HOT BOX

The second instrument used in this work for measuring heat flow through vacuum glazing was developed specifically for determining the thermal performance of fenestration systems. This instrument - the IRC environmental test facility (ETF) at the Institute for Research in Construction, National Research Council of Canada (NRC) is shown schematically in Figure 3, and has been described in detail by Elmahdy (1992). It is a large area guarded hot box with some special features, including a constant temperature baffle on the room (warm) side of the sample, and a wind machine connected to an oscillating matrix of tubes on the weather (cold) side.

The vacuum glazing sample tested in the ETF was placed in a polystyrene mask wall, which is located within a polystyrene surround panel separating the warm and cold sides of the instrument. A feature of the ETF is the ability to determine accurately the heat transfer coefficients at both warm and cold surfaces of the sample. For example, on the warm side, the constant temperature baffle accurately defines the conditions for radiative heat transfer to the surface. In addition, convection heaters result in highly uniform air temperature within the hot box. On the cold side, the oscillating matrix of tubes is designed to provide uniform film heat transfer coefficient and stable air flow perpendicular to the surface of the glazing.

The actual values of heat transfer coefficients on the warm and cold sides of the instrument are determined by performing measurements on a calibration sample. This sample consists of a slab of polystyrene, 11 mm in thickness, sandwiched between two glass sheets, each 3.2 mm thick. The thermal conductance of the polystyrene core of the calibration sample is determined by guarded hot plate measurements. In the calibration procedure, the temperatures of the external surfaces of this sample are determined from measurements obtained with an array of fine thermocouples attached to the inner surfaces of the two glass sheets. The radiative heat transfer coefficient on the warm side is obtained from a knowledge of the surface emittances of the glass sheet and the constant temperature baffle. The convective heat transfer coefficient can thus be determined, including its dependence on the power transmitted through the sample. The heat flow through the mask wall is estimated from measurements of the surface temperatures of this panel and a knowledge of its thermal resistance, obtained from guarded hot plate measurements. Corrections are made for additional flanking losses, associated with heat flow through the mask wall near the edge of the calibration sample. Great care is taken to eliminate air leakage between opposite sides of the sample.

An uncertainty analysis of the ETF has been made by Elmahdy (1992), including effects of errors in the measured temperatures, the thermal resistance of the calibration sample, the surface film coefficients, and the flanking losses. It has been concluded that the accuracy of measurements of the heat flow through the sample of vacuum glazing, 1 m $\times$ 1 m in size, is approximately ±6%.

In the tests on the sample of vacuum glazing, thermocouples were attached at various points on both sides. Although this is not normally done for standard tests with the ETF, it was felt that useful data could be obtained due to the unusual nature of the vacuum glazing sample. The tips of the thermocouples were located at the mid-points of unit cells of the pillar array. As has been discussed above, the surface temperatures at these locations are very close to the average center-of-glazing surface temperatures of the glass sheets.

4. MEASUREMENTS OF HEAT TRANSFER THROUGH A SAMPLE OF VACUUM GLAZING

In this section, test data, which were obtained from both measurement techniques discussed above on a sample of vacuum glazing, are presented and the results are compared.

4.1 DESCRIPTION OF SAMPLE

The vacuum glazing measured in this work was an experimental sample fabricated in the Department of Applied Physics at The University of Sydney. The construction of the sample is illustrated in Figure 1. The glazing is made from two sheets of 4 mm thick soda-lime glass. The larger sheet is 999 mm $\times$ 998 mm in size; the other sheet is 3 mm smaller all round. The solder glass edge seal extends a distance of approximately 8 mm inwards from the external edge of the larger sheet. The dimensions of the evacuated region are therefore 983 mm x 982 mm (area = 0.965 m^2).

The support pillars, which separate the glass sheets, are fabricated from Inconel 718. The pillars are made from a sheet of this material, 0.15 mm thick, using a double-sided photolithographic process and an electrochemical etching technique. This results in some variation in the size and shape of the surfaces of the pillars, which contact the glass. However, the average area of the contact regions is equal to that of a circle, 0.25 mm in diameter. The support pillars are placed on a square grid, separated by 25 mm. The heat transfer coefficient due to conduction through the array of support pillars can therefore be calculated from Equation 6 to be equal to 0.40 W/(m^2 K).

In the center of the sample, the pillars are displaced outwards slightly to give a pillar-free region, approximately 50 mm in diameter. This permits an accurate measurement with the small area guarded hot plate apparatus to determine the heat transfer coefficient due to radiation and residual gas.

The two glass sheets have pyrolitically deposited low emissivity coating on the internal (evacuated) surfaces of the glass. The effective radiative and gas heat transfer coefficient was measured in the guarded hot plate apparatus to be 0.81±0.01 W/(m^2 K) for temperatures of the internal surfaces of the glass sheets of 23.10°C and 3.38°C. This value is typical of that which has been obtained on many similar samples of vacuum glazing for which gaseous conduction has been shown to be negligible. This heat transfer coefficient can be used with Equations 2 and 3 to calculate the emittance of each of the internal surfaces. The value obtained in this way is 0.26. This is considerably higher than the typical value of 0.20 for the emittance of the as-received glass, measured in the same way. This difference is due to degradation of the coatings during the high temperature process for forming the solder glass edge seal.

The guarded hot plate measurement of radiative heat transfer coefficient is accurate to ±1%. However, measurements on individual, as-received samples of low emittance glass have shown point-to-point differences of up to ±5%. In the calculation of heat transfer through the glazing, a radiative heat transfer coefficient of 0.81±0.04 W/(m^2 K) was therefore used to account for the effect of such variability.

4.2 COMPARISON BETWEEN LOCAL AND OVERALL MEASUREMENTS OF HEAT TRANSFER

Table 1 lists the conditions under which measurements were made in the NRC hot box. Three separate tests were made, at progressively lower cold air temperatures. The overall heat transfer data contain a component due to flanking losses through the polystyrene surround panel. Estimates of these flanking losses, based on data from Elmahdy (1992), are included in Table 1, and were used to calculate the overall heat flow *through the glazing* for the three separate test conditions.

Table 1 also includes estimates of the boundary (warm and cold side) heat transfer coefficients on both sides of the glazing unit, obtained from independent measurements on a Calibration Transfer Standard (CTS) sample. These coefficients were used in the finite difference model, together with the temperature-adjusted radiative heat transfer coefficient calculated from Equation 4, and the estimate of the pillar array heat transfer coefficient due to conduction obtained from Equation 6, to calculate the overall heat transfer through the glazing on the basis of local U-value data. In these calculations, it was necessary to perform two or three iterations, correcting each time for the temperature dependence of radiative heat transfer coefficient as defined in Equation 4. Values of overall heat flow obtained in this way are also shown in Table 1; the two estimates agree to well within experimental error. The principal contribution to the uncertainty in the estimated heat flows is associated with the allowance made for point-to-point variability in the emittance of the doped tin oxide coatings.

It is instructive to determine the contributions to the overall heat flow through the glazing from the various sources discussed above. Table 2 shows approximate estimates for these separate contributions for the three test conditions. These estimates were obtained by using the method outlined in Sections 2.5 and 2.6 above. The radiative heat transfer coefficient was calculated from the experimental guarded hot plate data, corrected for the measured values of surface temperature using Equation 4. The total, center-of-glazing U-value was obtained by combining the radiative and pillar array heat transfer coefficients. These were then used to determine the gross heat flow $Q_{radiation+pillars}$ through the area (0.965 m^2) of the evacuated region of the sample. The effect of the edge conduction on this quantity was accounted for by reducing this heat flow by an amount corresponding to an area of width equal to one characteristic distance around the edges (23 mm), as described in Section 2.5. This gives the net total radiative and pillar heat flow. To this quantity is added the lateral heat flow along the glass sheets and through the edge seal $Q_{lateral\ flow}$ (as determined from the simple solution to the one dimensional analytic model), and the heat flow through the exposed area of the solder glass edge seal Q_{edge} (which for simplicity, is assumed to be plane parallel). The sum of these heat flows is the total heat flow Q_{total} through the glazing.

There are several points of interest about the results presented in Table 2. Firstly, the total heat flows obtained from this simple approach are in good agreement with the results in Table 1, which were obtained from the finite difference solution to the analytic model. Secondly, the measured values of surface temperatures of the glazing can be combined with the total radiative and pillar array heat transfer coefficient, to obtain independent estimates of the magnitudes of the heat transfer coefficients at both external surfaces. These results are in very close agreement with the values given in Table 1, which were obtained from the independent calibration procedure. Finally, the results in Table 2 give insights into the relative magnitudes of the different contributions to the total heat flow through the glazing Q_{total}. As expected, the largest contribution to the total heat flow is due to radiation and pillar conduction. However, nearly one third of the total heat flow is due to lateral conduction along the glass sheets near the edge seal. In addition, the decrease in radiative and pillar heat flow due to the reduced temperature difference in this edge region is quite large - approximately 10% of the total heat flow is due to these two effects. Finally, about 10% of the total heat flow are through the uninsulated solder glass edge seal.

5. DISCUSSION AND CONCLUSION

It is very gratifying that the measurements of heat flow made with the ETF agree so well with estimates based on local heat transfer data. The results confirm that it is acceptable to add the separate contributions to the heat flow from the pillars and radiation, ignoring any interactions between them. It is further concluded that the simple one-dimensional approach for estimating the effects of lateral heat flow near the edge seal gives a very good estimate for the additional heat flow due to this effect.

The results quoted in this paper are for a particular design of vacuum glazing, mounted in a certain way in a guarded hot box, and measured under specific conditions. The external measurement conditions are, in fact, representative of what might be encountered in practical, cold-climate applications, and indeed are not too dissimilar from "standard" winter conditions in some of the measurement standards. The method of mounting the sample, however, is not one, which would ever be used in practice. The solder glass edge seal would always be enclosed within a window frame, which would usually be made of relatively well-insulating material. The contribution to the total heat flow through the glazing due to direct conduction through the edge seal (~10% of the total heat flow) would therefore almost certainly be reduced in a practical installation. Furthermore, extending the window frame a short distance beyond the edge seal would result in additional useful reductions in the overall heat transfer.

Finally, it should be noted that there are many design options for vacuum glazing, which can either increase, or decrease the overall heat flow through the unit. For example, use of thinner glass requires that the pillars be more closely spaced, resulting in an increase in pillar conduction. This can be partially offset by the lower compressive stress in the pillars which permits the use of smaller pillars with increased thermal resistance; in addition there is some reduction in the magnitude of the lateral heat flow near the edges for thinner glass. There are also very real prospects for substantially reducing the radiative heat transfer through vacuum glazing if lower emittance coatings can be produced which will survive the high temperature edge sealing process. Coatings with emittances as low as 0.04 are becoming available for application with glass that is to be tempered or bent. It is possible that the design principles used to produce these coatings may also result in the development of very low emittance coatings that will be useful in vacuum glazing.

Whatever the future directions for the design of vacuum glazing, the results of this paper confirm that it is possible to make accurate estimates of the overall heat flow through such glazings by combining the effects of the separate internal heat transfer processes - radiation and pillar conduction between the two glass sheets, and lateral heat flow in the vicinity of the edge seal - with known heat transfer coefficients at the boundaries of the unit surfaces.

REFERENCES

ASTM. 1991. *Standard procedures for determining the steady state thermal transmittance of fenestration systems. ASTM E 1423-91*. Philadelphia: American Society of Testing and Materials.

Collins, R.E., C.A. Davis, C.J.Dey, S.J.Robinson, J-Z. Tang and G.M.Turner. 1993. Measurement of local heat flow in flat evacuated glazing. *International Journal of Heat and Mass Transfer* **36**, 2553-2563.

Collins, R.E. and T.M. Simko. 1998. Current status of the science and technology of vacuum glazing. *Solar Energy*, in press.

Elmahdy, A.H. 1992. Heat transmission and R-value of fenestration systems using IRC hot box: procedure and uncertainty analyses. *ASHRAE Transactions* 98, 630-637.

Holm, R. 1979. *Electrical contacts, theory and application,* 4th edn. Springer-Verlag, Berlin.

Pilkington, 1989. Pilkington K Glass information sheet. Pilkington Glass Limited, England.

Robinson, S.J. and R.E. Collins. 1989. Evacuated windows - theory and practice. *ISES Solar World Congress*, *International Solar Energy Society*, Kobe, Japan.

Turner, G.M., R.E. Collins, G.R. Facer and M.A. Scheumack 1994. Outgassing effects in evacuated glazing. In *Proceedings of the SPIE International Symposium on Optical Materials Technology for Energy Efficiency and Solar Energy Conversion XIII*, Freiburg, Germany.

Simko, T.M. 1996. Heat transfer processes and stresses in vacuum glazing. *Ph.D. Thesis*, The University of Sydney.

Simko, T.M., R.E. Collins, Beck and D. Arasteh. 1995. Edge conduction in vacuum glazing. In *Proceedings of Thermal Performance of the Exterior Envelope of Buildings IV, Heat Transfer in Fenestration II*, Geshwiler M., Alger J., Moran M. (Eds), pp. 601-611, Florida, USA.

Zhang, Q.-C., T.M. Simko, C.J. Dey, R.E. Collins, G.M. Turner, M. Brunotte and A. Gombert. 1997. The measurement and calculation of radiative heat transfer between uncoated and doped tin oxide coated glass surfaces. *International Journal of Heat and Mass Transfer*, 40: 61-71.

Zoller, F. 1924. Hollow pane of glass. *German Patent No. 387 655*.

Table 1 Test data for measurement of 1 m × 1 m sample of vacuum glazing in the NRC guarded hot box.

Test number	Air temperature (°C)		Heat transfer coefficient (W/(m^2 K))		Measured total heat flow through unit (W)	Flanking losses (W)	Measured net heat flow through glazing (W)	Estimate of heat flow from FDM (W)
	Warm side	Cold side	Warm side	Cold side				
1	22.7	-7.1	7.3	25.2	43.7	1.7	42.0±2.5	41.9
2	23.2	-12.3	7.3	25.2	51.9	2.2	49.7±3.0	49.4
3	23.9	-17.5	7.5	25.2	60.9	2.7	58.2±3.4	58.2

Table 2 Approximate estimates of contributions to heat flow through vacuum glazing for the NRC measuring conditions, obtained from the analytic model.

Test Number	Glass temperature (°C)		$\Delta T_{glass\text{-}glass}$ (°C)	$\bar{T}$ (K)	$C_{radiation}$ W/(m^2 K)	C_{total} W/(m^2 K)	Gross $Q_{radiation+pillars}$ through 0.965 m^2 (W)	Reduction of $Q_{radiation+pillars}$ near edge (W)	Net $Q_{radiation+pillars}$ (W)	$Q_{lateral\ flow}$ (W)	Q_{edge} (W)	Q_{total} (W)
	Warm side	Cold side										
1	18.9	-6.0	24.8	279.4	0.73	1.13	27.2	2.7	24.5	13.2	4.0	41.7
2	18.7	-11.0	29.7	276.8	0.71	1.11	31.8	3.2	28.6	15.8	4.8	49.2
3	18.8	-16.0	34.8	274.3	0.69	1.09	36.6	3.7	32.9	18.4	5.7	57.0

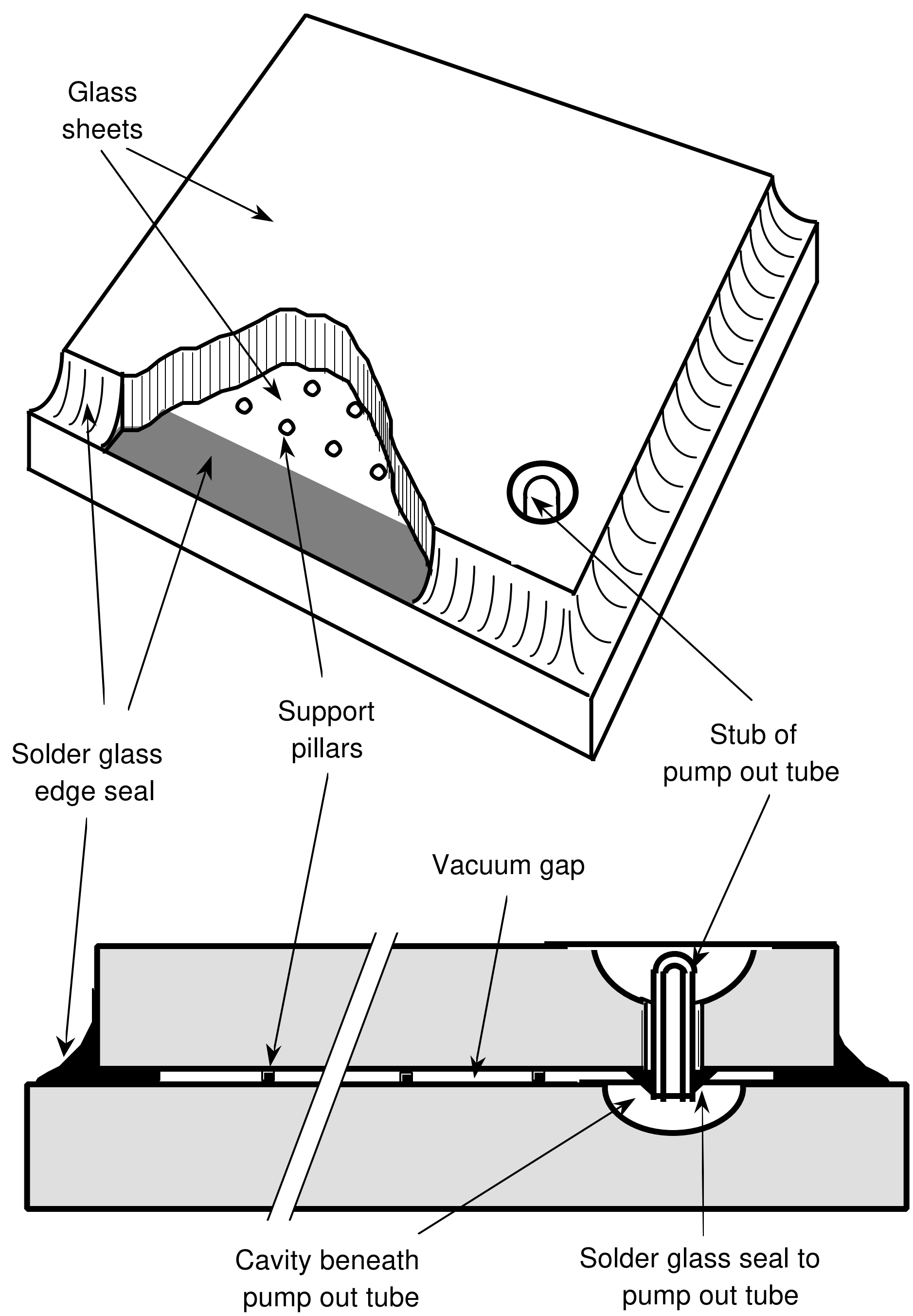

Figure 1 Vacuum glazing

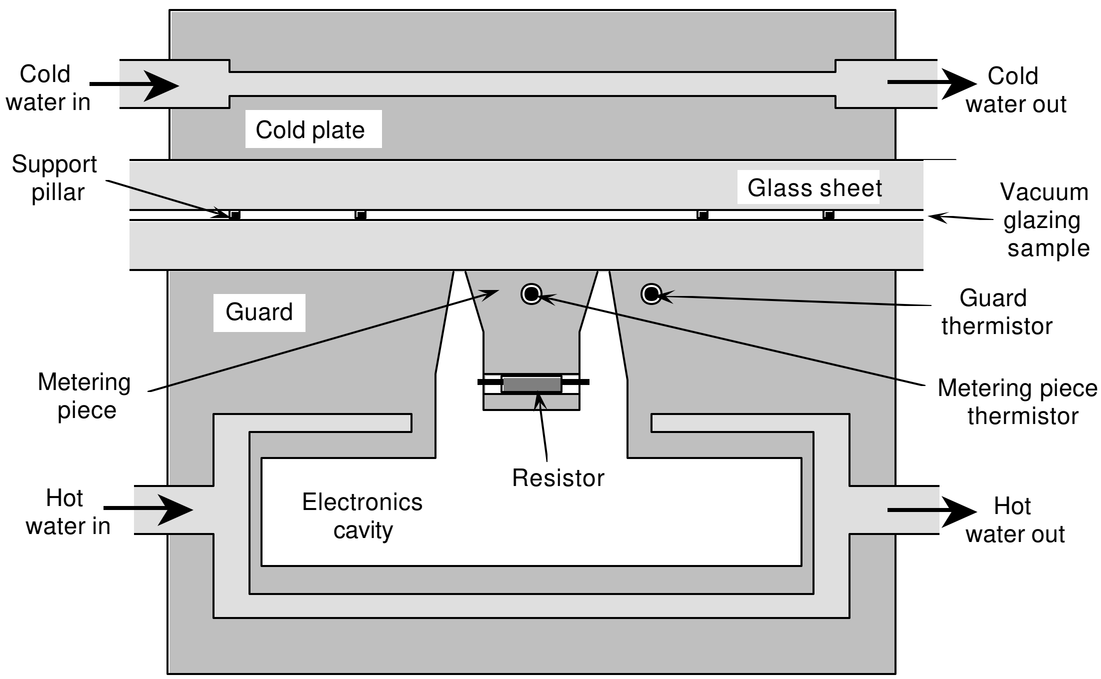

Figure 2 Small area guarded hot plate

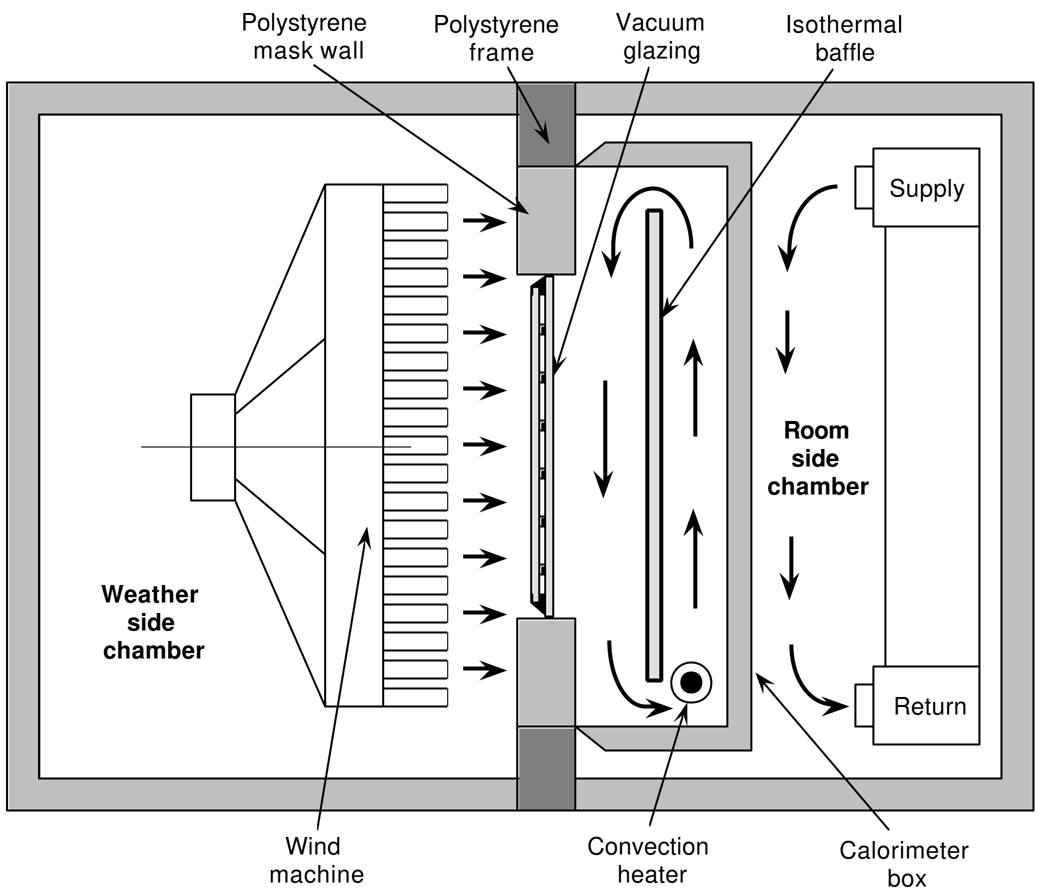

Figure 3 Environmental Test Facility

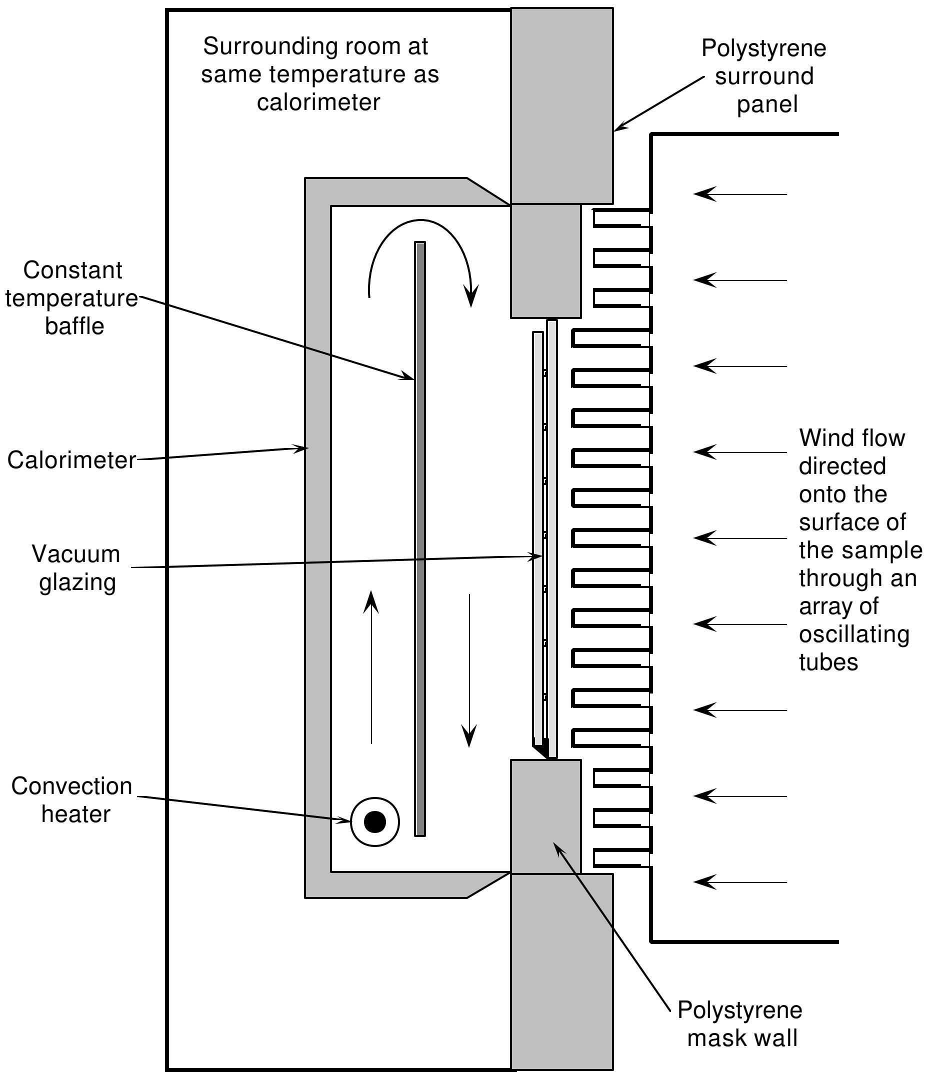
Surrounding room at
same temperature as
calorimeter
Polystyrene
surround
panel
Constant
temperature
baffle
Calorimeter
Vacuum
glazing
Convection
heater
Wind flow
directed
onto the
surface of
the sample
through an
array of
oscillating
tubes
Polystyrene
mask wall